ORIGINAL ARTICLE

Antioxidant, anti-lipidemic, hypoglycemic and antiproliferative effects of phenolics from Cortex Mori Radicis

Chao Li [a,1], Yao Peng [b,1], Wei Tang [a], Teng Li [a], Mansour K. Gatasheh [c], Rabab Ahmed Rasheed [d], Junning Fu [e], Juping He [a], Wei-dong Wang [a], Yingbin Shen [b], Yichao Yang [f], Yongsheng Chen [e,*], Arshad Mehmood Abbasi [g,h,*]

[a] College of Food and Bioengineering, Xuzhou University of Technology, Xuzhou, Jiangsu, 221018, China
[b] School of Life Sciences, Guangzhou University, Guangzhou 510006, China
[c] Department of Biochemistry, College of Science, King Saud University, Riyadh 11451, Saudi Arabia
[d] Histology & Cell Biology Department, Faculty of Medicine, King Salman International University, South Sinai, Egypt
[e] Department of Food Science and Engineering, Jinan University, Guangzhou 510632, China
[f] School of Public Health, Guangzhou Medical University, Guangzhou 511436, China
[g] Department of Environmental Sciences, COMSATS University Islamabad, Abbattabad Campus 22060, Pakistan
[h] University of Gastronomic Sciences, Piazza Vittorio Emanuele II, 9, 12042 Pollenzo, Italy

Abstract Cortex Mori Radicis (CMR) is enriched in various phenolics, this study aimed to estimate the antioxidant effect, enzyme (lipase, α-amylase, α-glucosidase and acetyl-cholinesterase) inhibition and the anti-proliferative effect of the phenolic compounds in CMR. However, the amount of these compounds obtained from CMR is highly dependent on the processing conditions. In this study, the processing parameters of extracting the phenolics from CMR using ultrasonic technique pooled with high-speed shearing extraction (UTPHSE) were optimized. Subsequently, the phenolics from Cortex Mori Radicis (PCMR) were purified using AB-8 macroporous resin, and their chemical analysis, antioxidant, enzyme inhibition, and antiproliferative activities were studied. Based on our findings, the optimal parameters of UTPHSE were: L/S ratio 25.8:1 (mL/

* Corresponding authors at: Department of Environmental Sciences, COMSATS University Islamabad, Abbattabad Campus 22060, Pakistan (A.M. Abbasi).
E-mail addresses: 11185@xzit.edu.cn (C. Li), 2111914037@e.gzhu.edu.cn (Y. Peng), tangwei@xzit.edu.cn (W. Tang), mgatasheh@ksu.edu.sa (M.K. Gatasheh), fujunning@jnu.edu.cn (J. Fu), 10227@xzit.edu.cn (J. He), wwd@xzit.edu.cn (W.-d. Wang), shenybin@gzhu.edu.cn (Y. Shen), chysh11@126.com (Y. Chen), amabbasi@cuiatd.edu.pk (A.M. Abbasi).
[1] These authors contributed equally to this work.

g), voltage 81.0 V, ultrasonic temperature 51.8 ℃ and ultrasonic time 289 s. And under the optimal extraction conditions, the extraction rate of the PCMR was 0.531 ± 0.004%. Compared with PCMR, the contents of "total phenolics, flavonoids, flavonols, flavanols and phenolic acids" increased 2.30, 2.67, 2.59, 3.63 and 2.72 times in the purified phenolics from Cortex Mori Radicis (PPCMR), respectively. In addition, PPCMR depicted significant DPPH, $ABTS^+$ and superoxide anion radicals' scavenging capability, reducing power, ferric ion reducing antioxidant power (FRAP) and remarkable inhibitory activities on "lipase, alpha-amylase, alpha-glucosidase, and the proliferation of HeLa, HepG2 and NCI-H460". At the same time, the morphological changes of HeLa, HepG2 and NCI-H460 cells suggested that PPCMR could effectively inhibit the proliferation of tumor cells in vitro. Therefore, PPCMR have good potential as natural antioxidants, antilipidemic, hypoglycemic, and antineoplastic agents in functional foods and pharmaceuticals.

1. Introduction

The white mulberry "*Morus alba* L.", the black mulberry "*M. nigra* L." and the red mulberry "*M. rubra* L." are three common species of the genus Morus, family Moraceae (Ercisli and Orhan, 2006). Among these, *M. alba* is native to northern China and widely cultivated in Europe, North America, South America and Africa (Imran et al., 2010; Paola et al., 2009). According to the Chinese pharmacopeia, fruits, leaves and root bark of *M. alba* have been used as traditional Chinese medicines for thousands of years. Most of the previous studies were focused on food and medicinal applications of the leaves and fruits of *M. alba*. Specifically, its leaves have been widely reported for making tea or as food for silkworms to produce yarn (Hisato et al., 2008), and use of fruits in making health drinks in east Asian countries (Huang et al., 2020). The root bark of *M. alba* is also known as Cortex Mori Radicis (CMR), is a rich source of phenolics (Čulenová et al., 2020), flavonoids (Zheng et al., 2010), coumarins (Syah et al., 2004), triterpenoids (Ferrari et al., 2000) and alkaloids (Asano et al., 2001). As a traditional herbal medicine, CMR has been commonly used in China as anti-asthmatic, to reduce blood pressure and to treat cardiovascular diseases and diabetes (Kim et al., 2011; Shibata et al., 2007; Yang et al., 2010).

Phenolics possess significant antioxidant, enzyme inhibitory and antitumor activities (Hu et al., 2020; Wu et al., 2020). Deghima et al. demonstrated that various antioxidant activities (antiradical, iron-chelating ability, reducing power and lipid peroxidation) of the root extract of Ranunculus macrophyllus were highly related to the contents of polyphenolics (Deghima et al., 2020). Likewise, polyphenols from young apple, tomato and lotus seed extracts depicted significant potential in α-glucosidase and acetylcholinesterase inhibition and anti-proliferative activities against HepG2 cell (Blaszczak et al., 2020; Tian et al., 2020; Yan et al., 2019). These findings revealed that phenolics have a variety of biological activities. Dipayan Sarkar and Kalidas Shetty 2014 found that human body cannot synthesize the phenolics, and often obtained from natural resources such as fruit, vegetables, medicinal plants and grains, etc. (Zou et al., 2017). Therefore, an efficient extraction method of phenolics plays an important role in their biological activity value. High-speed shearing extraction (HSE), is a highly efficient, environmentally friendly and energy saving novel technology for extracting active ingredients from plants (Song et al., 2019; Zhong et al., 2019). The principle of HSE is to use the high-speed rotating rotor in a solution to produce cavitation, mechanical and shear effects to rapidly dissolve the substances in plant cells to achieve balance.

Ultrasonic-assisted extraction process is the synergistic effect of cavitation, mechanical and thermal effects (Liu and Yang, 2018). The high intensity of the ultrasonic wave in the solvent causes pressure fluctuations, and the instantaneous generation of many vacuum cavitation bubbles (Rao and Rathod, 2015). These bubbles suddenly implode within a few milliseconds, accompanied by local temperature and pressure rise, which is conducive to the solvent penetration in plant cells and to improve the extraction effect (Teh and Birch, 2014). The above two methods have been widely used to extract active ingredients such as polyphenol (Guo et al., 2017), flavonoids (Cheng et al., 2016; Garcia-Castello et al., 2015), and polysaccharides (Lin et al., 2018). Yet, there is limited data about the extraction of phenols from "CMR" using "ultrasonic technology combined with high-speed shear extraction (utphse)". Ultrasonic power installed to 250 W. Therefore, the objectives of this study were to: (a) to optimize the UTPHSE of the phenolics from CMR, (b) to purify the phenolics using AB-8 macroporous resin, (c) to study the composition of the purified phenolics from Cortex Mori Radicis (PPCMR) and their biological activities in vitro including antioxidant, enzyme inhibitory "lipase, alpha-amylase, alpha-glucosidase and acetylcholinesterase", and anti-proliferative activities against various cancer cells' lines.

2. Materials and methods

2.1. Sampling

CMR was purchased from Limin Herbal Pieces Co., Ltd. (Chengdu, Sichuan, China). After proper taxonomic recognition, specimen were submitted in the herbarium of Xuzhou University of Technology, under voucher number No. 20180322–1.CMR is dried at 60 °C in a GZX-9070MBE oven (Boxun, Shanghai, China), then uniformly ground to a fine powder using a WKX-160 mill (QingzhouJingcheng, Shandong, China), sieved through a 60 mesh sieve and stored at −20 °C.

2.2. Chemicals and reagents

Gallic acid (≥98%), rutin (≥98%), catechin (≥98%), caffeic acid (≥98%), ascorbic acid, 2,2-diphenyl-1-picrylhydrazyl (DPPH, D9132, ≥98.0%), porcine pancreatic lipase (Type II, EC 3.1.1.3; L3126), porcine pancreatic α-amylase (Type VI-B, EC 3.2.1.1, A3176), saccharomyces cerevisiae α-glucosidase (EC 3.2.1.20, G3651), electrophorus electricus's acetyl-cholinesterase (electric eel) (Type VI-S, EC 3.1.1.7, C3389) and 3-(4,5-Dimethylthiazol-2-yl)-2,5-diphenyltetrazolium bromide (MTT, M5655, ≥97.5%) were acquired from Sigma-Aldrich Co., Ltd. (St. Louis, MO, USA). Cervical cancer cell line HeLa, liver tumor cell line HepG2, and lung carcinoma cell line NCI-H460 were acquired from the Cell Bank of the Committee for Typical Culture Conservation of the Chinese Academy of Sciences. Trypsin-EDTA solution and 5-

Fluorouracil (5-FU, F6627, $\geq$99%) were acquired from Beyotime Biotechnology Co. Ltd. (Shanghai, China). All chemicals were of analytical grade and acquired from Sinopharm Chemical Reagent Co., Ltd. (Shanghai, China), while Anhui Sanxing Resin Technology Co., Ltd. (Bengbu, Anhui, China) supplied the macroporous resin AB-8.

2.3. Preparation of PPCMR

2.3.1. Extraction

A sample powder of 30 g was accurately weighed, transferred into the extraction vessel (2.0 L) and immersed in 70% ethanol (v/v). The cutter head of high speeds shearing machine (ZHBE-50, Zhijing, Zhengzhou, Henan, China), was put into the extraction container, and the extraction container was put into the ultrasonic cleaning machine (SB-5200DTN, Xinzhi, Ningbo, Zhengjiang, China). After the high-speed shearing machine was turned on, the voltage began to gradually increase. When the voltage reached the preset voltage, the ultrasonic cleaner was turned on, and the ultrasonic power was set to 250 W and the extraction time was counted. After finishing the extraction process, the crude extracts were collected, filtered, concentrated and lyophilized for the further purification.

2.3.2. Purification

2 g of crude extract was mixed in deionized water (500 mL), and pH was adjusted to 4.6 using hydrochloric acid (1 M) for the dynamic adsorption test. The samples were loaded into a column filled with AB-8 macroporous resin (2.6 cm $\times$ 60 cm) and a bed volume (BV) of 320 mL at 1BV/h flow-rate and subjected to dynamic desorption experiments. Elution was done using distilled water until the solution becomes colorless, the final cleaning was then performed with 3.5 BV ethanol (70%) at a flow rate of 0.5 BV/hour. Afterwards, the colorless eluate was concentrated and lyophilized to analyze its chemical properties and in *vitro* biological activities.

2.4. Determination of extraction rate

Extraction rate of the total phenolics was determined using the equation:

$$\text{Extraction rate}(\%) = \frac{W_e}{W_t} \times 100 \tag{1}$$

where: W_e symbolizes the amount of gallic acid equivalents recovered from the solution and W_t represents the amount of CMR.

2.5. Optimization

We examined the effects of ethanol volume fraction, liquid–solid ratio, voltage, ultrasonic temperature and time. The four-factor, three-level Box-Behnken experiment was used to estimate ideal extraction conditions of UTPHSE by selecting four significant factors, namely, liquid–solid ratio (x_1, 20–30 mL/g), voltage (x_2, 70–90 V), ultrasound temperature (x_3, 40–60 °C), and ultrasound time (x_4, 240–320 mL/g), based on the previous one-factor experiments. Design-Expert V 8.0.6 Trial software was used to evaluate the trial data State-Ease, Inc., Minneapolis MN, USA. Response surface analysis is based on the Eq. (2) using a generalized second-order polynomial model:

$$\text{Extraction rate}(\%) = \beta_0 + \sum_{i=1}^{4} \beta_i x_i + \sum_{i=1}^{4} \beta_{ii} x_i^2 + \sum_{i=1}^{3}$$
$$\times \sum_{j=i+1}^{4} \beta_{ij} x_i x_j \tag{2}$$

where: β_0 represent constant coefficient; β_i, β_{ij} and β_{ii} demonstrating the coefficient's regression for linear, interaction and quadratic terms; x_i and x_j are the actual values of independent variables.

2.6. Phytochemical analysis

The total phenolics was estimated using the modified as described previously (Xiang et al., 2019). Gallic acid was used for the calibration, and the final value were reported as mg GAE/g.

The total flavonoids was determined based on Benabderrahim et al. (Benabderrahim et al., 2019). Rutin was used for the calibration, and the final value were reported as mg RE/g.

The total flavonols was estimated using the modified method as described previously (Oyedeji-Amusa and Ashafa, 2019). Rutin was used for the calibration, and the final value were reported as mg RE/g.

The total flavanols content was enumerated based on Jiao et al. (Jiao et al., 2018). Catechols was used for the calibration, and the total flavonoids content was presented as mg CE/g.

The total phenolic acids' content was enumerated following previously described method of Timur Hakan Barak et al. (Barak et al., 2019). Caffeic acid was used for the calibration, and the final values were presented as mg CAE/g.

2.7. Antioxidant assays

2.7.1. DPPH radical scavenging assay

The DPPH inhibition potential of PPCMR was determined using the previously described the method (Zdunić et al., 2020). Precisely, various concentrations of PPCMR (50 μL) and 150 μL of DPPH (0.15 mM) were mixed in 96 well plates, and kept for 60 min (in dark) at 37 °C. The absorbance was measured with a microplate reader (Synergy H1, Bio-Tek. Winooski, VT, USA) at 517 nm. Positive control was ascorbic acid and DPPH scavenging activity was intended using the formula (3):

$$\text{scavenging activity}(\%) = \left(1 - \frac{A_s}{A_c}\right) \times 100 \tag{3}$$

where: A_s represents sample absorbance, A_c indicates absorbance of blank

2.7.2. ABTS$^+$ scavenging assay

The inhibition potential of PPCMR towards ABTS radical was estimated by previously modified (Cătunescu et al., 2018). First, ABTS + radicals were prepared by mixing 5 mL of 7 mM ABTS solution with 88 μL of 140 mM potassium persulfate solution. Then, it was incubated for 12–16 h at its absorbance was adjusted to 0.85 $\pm$ 0.02 at 734 nm. Dif-

ferent concentrations of PPCMR (40 μL each) and ABTS radical solution (160 μL) were mixed in a 96-well plate, and kept in the dark at 37 °C for 60 min. The absorbance was then measured at 734 nm using a microplate reader. Final values were calculated by the formula (3), while ascorbic acid was the positive control:

2.7.3. Scavenging activity of superoxide anion

The superoxide anion radical scavenging potential of PPCMR was estimated by previously modified (Lei et al., 2019). Shortly, 20 μL of different concentrations of PPCMR and 100 μL of 50 mM Tris-HCl buffer (pH 8.20) were mixed in well plates and kept in the dark for 20 min at 37 °C. Afterwards, 8 μL of 3 mM pyrogallol (in 10 mM HCl) was injected into each well plate and kept in the dark at 37 °C for 5 min. Afterwards, 32 μL of 1 M hydrochloric acid was mixed to stop the process, and the absorbance was measured at 320 nm using a microplate reader. The final values were calculated using the Eq. (4), while ascorbic acid was the positive control:

$$\text{scavenging activity}(\%) = \left(1 - \frac{A_s - A_{sb}}{A_c}\right) \times 100 \qquad (4)$$

where: A_s is the absorbance of sample group, A_{sb} is sample background group absorbance, and A_c represents absorbance of the blank control.

2.7.4. Reducing power assay

Ferric ion reduction capacity PPCMR, was evaluated by the previously described colorimetric method (Gali and Bedjou, 2018). Precisely, different concentrations of PPCMR (10 μL each), 25 μL phosphate buffer (0.2 M, pH 6.6, PBS), and 1% w/v potassium ferricyanide (25 μL) were mixed in well plates. The reaction was then stopped by adding 25 μL of trichloro-acetic acid (10% w/v) and incubated for 20 min at 37 °C. After centrifugation, 85 μL of distilled water and 17 μL of ferric chloride (0.1% w/v) were added to the supernatant, and the absorbance was measured at 700 nm using a microplate reader. The final values were calculated using the equation (5), while ascorbic acid was the positive control:

$$A_{rp} = A_s - A_c \qquad (5)$$

where: A_{rp} is the reducing power, A_s and A_c indicate absorbance sample and control groups.

2.7.5. Ferric ion reducing antioxidant power (FRAP) assay

Reduction of ferric ion by PPCMR was anticipated using the method of Alves et al. (Alves et al., 2019). First, FRAP reagent was prepared by mixing 10 mM TPTZ (2,4,6-tripyridyl-s-triazine) with 40 mM HCl, ferric chloride (20 mM) and 0.3 M Macerate buffer (pH 3.6) at a ratio of 1:1:10, respectively. The 96-well plates were added with 185 μL of FRAP reagent and 15 μL of different concentrations of PPCMR, and incubated for 10 min in the dark at room temperature. The absorbance was measured at 593 nm using a microplate reader. FRAP(A_{frap}) values were calculated using the Eq. (5), while ascorbic acid was the positive control.

2.8. Enzyme inhibition assays

2.8.1. Inhibition of lipase

The inhibition potential of PPCMR for active lipase was estimated using a modified method previously reported (Marilena et al., 2019). Concisely, different concentrations of 50 μL of PPCMR were mixed with an equal volume of 1.2 U/m lipase solution in 0.1 M PBS (pH 8.0) in well plates, and incubated in the dark for 10 min at 37 °C. Afterwards, 100 μL of p-nitrophenyl palmitate (0.2 mM, PBS) was added and kept in the dark again under the same conditions. The absorbance was measured at 405 nm using a microplate reader (Synergy H1, Bio-Tek. Winooski, VT, USA). The inhibition rate of lipase was estimated using the equation (6) with orlistat as a positive control:

$$\text{Lipase inhibition rate}(\%) = \left(1 - \frac{A_s - A_{sb}}{A_n - A_{nb}}\right) \times 100 \qquad (6)$$

where: A_s is the absorbance of sample, A_{sb} is the absorbance of sample background group, A_n indicates absorbance of negative control, and A_{nb} is the absorbance of negative background control group.

2.8.2. Alpha-amylase inhibitory assay

The inhibition potential of PPCMR against α-amylase activities was determined by previously modified (Yuan et al., 2018). Briefly, 700 μL of different concentrations of PPCMR was mixed with 600 μL of soluble starch in a test tube and incubated in the dark for 5 min, then 200 μL of 20 U/ml α-amylase solution and 1% (m) 500 μL of dinitrosalicylic acid were added and incubated in the dark at 100 °C for 5 min. Cool to room temperature, dilute to 10 mL with deionized water, inoculate 200 μL of sample into a 96-well plate and measure absorbance at 540 nm using a microplate reader. The inhibition rate of α-amylase was estimated using Eq. (6) with acarbose as a positive control.

2.8.3. Inhibition of alpha-glucosidase

The inhibitory potential of PPCMR against the activity of α-glucosidase was estimated using the method as described previously (Zhang et al., 2020). Shortly, 40 μL of different concentrations of PPCMR was mixed with an equal volume of 5 mM p-nitrophenyl-D-glucopyranose (pH 7.0) in 0.1 M PBS and incubated for 10 min at 37 °C in the dark in a 96-well plate. Afterwards, 20 μL of α-glucosidase (40 U/mL in PBS) was mixed into the above mixture. Incubate again for 20 min under the same conditions and add 100 μL of sodium carbonate (0.3 mM). The absorbance was measured at 405 nm using a microplate reader, and inhibition rate of α-glucosidase was estimated using equation (6) with acarbose as a positive control.

2.8.4. Inhibitory assay for acetyl-cholinesterase activity

The acetyl-cholinesterase inhibitory potential of PPCMR was estimated using the modified method as described earlier (Zdunić et al., 2020). Various concentrations of PPCMR (100 μL each) were mixed with 20 μL of acetylcholinesterase

(0.2 U/mL in 0.1 MPBS, pH 8.0) in a 96-well plate, and incubated in the dark at 37 °C for 15 min. Afterwards, 40 μL each of 5,5′-dithiobis (2-nitrobenzoic acid) (1 mM in PBS) and acetylthiocholine iodide (1.87 mM in PBS) were added to the above mixture and kept at 37 °C for 20 min in the dark. Absorbance was measured at 405 nm, and the inhibition rate of acetylcholinesterase was calculated using equation (6) with galantamine as a positive control.

2.9. Antiproliferative assays

2.9.1. Cell culture

Different cancer cell lines viz. cervical carcinoma cells (HeLa), Hepatoma or liver cancer cells (HepG2) and lung cancer cells (NCI-H460) were cultured in RPMI-1640 media containing heat-inactivated 10% FBS (Fetal bovine serum), 100 units/mL, and 100 g/mL streptomycin. Cell culture was carried out in Jiangsu Food Safety Biochip Testing Technology Engineering Laboratory, Xuzhou University of Technology, China. Cultured cells were kept in a moistened atmosphere with 5% CO_2 at 37 °C.

2.9.2. Cell viability assay

The succinate dehydrogenase activity (MTT assay) was estimated using the method as described previously with slight modifications to evaluate the anti-proliferative activities of PPCMR against HeLa, HepG-2 and NCI-H460 cells (Lu et al., 2018). In short, 100 μL of the cells at a density of 1×10^5 cells/mL and the same volume of PPCMR were mixed to achieve the final concentrations of 0, 14.06, 28.12, 56.25, 112.50, 225.00, 450.00, 900.00 μg/mL, respectively. Afterwards, the mixture was gently shaken for 1 min and incubated for 24 and 48 h at 37 °C with 5% CO_2 in a humidified incubator. After treatment, 5 mg/mL of MTT (20 μL) was mixed in PBS, and incubated in a humidified incubator with 5% CO_2 for an additional 4 h at 37 °C. The mixture was centrifuged, and the frozen cell precipitate was dissolved in 150 μL DMSO. After incubation, the absorbance was measured by using a microplate reader (Synergy H1, Bio-Tek, Winooski, VT, USA) at 490 nm. The inhibition rate of α-glucosidase was estimated using the Eq. (7) with 5-FU as a positive control:

$$\text{Inhibition rate}(\%) = \left(1 - \frac{A_s - A_b}{A_n - A_b}\right) \times 100 \qquad (7)$$

where: A_s donates sample group's absorbance, A_n is the negative control group's absorbance, and A_b is the blank control group's absorbance.

2.9.3. Cell morphological analysis

The cell proliferation analysis (MTT assay) was estimated using the method as described previously (Yang et al., 2019). In a 6-well culture plate, each well was inoculated with cell solution (2 mL), and incubated for 24 h under humid conditions at room temperature with 5% CO_2 before removing the previous medium. It was further divided into a sample control group, a model control group and a positive control group, and incubated at 37 °C for another 24 and 48 h. To compare the morphological changes of the cells, all groups of cells were observed by inverted microscopy TS100-F (Nikon, Chiyoda District, Tokyo Metropolitan, Japan) at ×400 magnification.

2.10. Statistical analysis

The data were analyzed using Design-Expert V8.0.6 software and results of the Box-Behnken design, 2-D contour and 3-D response surface plots were plotted. Origin V9.1 software was used to illustrate the findings of antioxidant, enzyme inhibition and antiproliferation assays, while SPSS V18.0 software was used to calculate 50% scavenging concentration (SC_{50}) on DPPH, $ABTS^+$ and superoxide anion radicals and the 50% inhibitory concentration (IC_{50}) on lipase, alpha-amylase, alpha-glucosidase and acetyl-cholinesterase. All data were expressed as mean ± standard deviation.

3. Results and discussion

3.1. Optimization of UTPHSE

3.1.1. Fitting the model

The interaction between four parameters including voltage, ultrasonic temperature, liquid to solid ratio and ultrasonic time (Table 1), was studied using Box Behnken experimental model, and multiple regression analysis was performed. The mathematical model was matched with the experimental data with the aim to find out an optimum range for the studied response. The following equation with coded values was used to describe the predicted model:

$$
\begin{aligned}
\text{Extraction rate } (\%) =\ & -5.951 + 7.185 \times 10^{-2}x_1 + 7.006 \times 10^{-2}x_2 \\
& + 4.282 \times 10^{-2}x_3 + 1.102 \times 10^{-2}x_4 - \\
& 9.5 \times 10^{-5}x_1x_2 + 3.1 \times 10^{-4}x_1x_3 + 5 \times 10^{-6}x_1x_4 + 9.5 \times 10^{-5}x_2x_3 \\
& + 1.375 \times 10^{-5}x_2x_4 + 3.75 \times 1\,0^{-6}x_3x_4 - \\
& 1.583 \times 10^{-3}x_1^2 - 4.707 \times 10^{-4}x_2^2 - 5.744 \times 10^{-4}x_3^2 - 2.153 \times 10^{-5}x_4^2
\end{aligned}
$$

$$(8)$$

As shown in Table 2, the significance of all coefficients is determined by the F-test and P-value. With the corresponding variables becoming more significant as the absolute P-value becomes smaller and the F-value becomes larger. The linear terms for liquid–solid ratio (x_1), voltage (x_2), and the interaction term of liquid–solid ratio and ultrasonic temperature (x_1, x_3) were seen to be significant at the 0.05 level, and the linear terms for ultrasonic temperature (x_3), ultrasonic time (x_4) and all quadratic terms were significant at the 0.001 level, whereas the other terms were insignificant. As mentioned in Table 2, the model was highly significant at $P < 0.0001$, the Lack of Fit ($P > 0.05$) was insignificant, and the predictive model had a predictive coefficient (R^2) of 0.9560 with an adequate accuracy of 13.978 (much greater than 4). Therefore, it was indicated that the predicted model is representative of the observed values, and could adequately explain the responses.

3.1.2. Response surface analysis

Predicting the effect of four variables on the extraction rate of PCMR by the regression model. The model generated tri-dimensional response surfaces and two-dimensional contour plots to show the link between the independent and dependent variables (Fig. 1 a-l). On one three-dimensional surface, two variables are represented, while the other two stays constant. The degree of contact was represented in the contour's form. The oval had a considerable impact, whereas roundness had no effect. The interaction between the liquid–solid ratio and ultrasonic temperature (x_1x_3) was excellent at the 0.05 level,

Table 1 Experiment results of Box-Behnken for the yield of PCMR.

No.	x_1	x_2	x_3	x_4	Extraction rate (%, Actual Value)	Extraction rate (%, Predicted Value)
1	20	70	50	280	0.417	0.414
2	30	70	50	280	0.433	0.443
3	20	90	50	280	0.444	0.443
4	30	90	50	280	0.441	0.453
5	25	80	40	240	0.393	0.401
6	25	80	60	240	0.426	0.434
7	25	80	40	320	0.428	0.429
8	25	80	60	320	0.467	0.467
9	20	80	50	240	0.428	0.427
10	30	80	50	240	0.436	0.445
11	20	80	50	320	0.463	0.455
12	30	80	50	320	0.475	0.477
13	25	70	40	280	0.397	0.402
14	25	90	40	280	0.394	0.403
15	25	70	60	280	0.427	0.419
16	25	90	60	280	0.462	0.457
17	20	80	40	280	0.415	0.415
18	30	80	40	280	0.428	0.405
19	20	80	60	280	0.406	0.420
20	30	80	60	280	0.481	0.471
21	25	70	50	240	0.433	0.424
22	25	90	50	240	0.447	0.432
23	25	70	50	320	0.438	0.443
24	25	90	50	320	0.474	0.474
25	25	80	50	280	0.514	0.525
26	25	80	50	280	0.530	0.525
27	25	80	50	280	0.524	0.525
28	25	80	50	280	0.524	0.525
29	25	80	50	280	0.532	0.525

Ratio of liquid to solid (x_1), voltage (x_2), ultrasonic temperature(x_3) and ultrasonic time (x_4).

Table 2 ANOVA results of quadratic regression model for response surface.

Source	SS	df	MS	F-value	P-value	Sig.
Model	0.046	14	3.275×10^{-3}	21.74	< 0.0001	***
x_1	1.220×10^{-3}	1	1.220×10^{-3}	8.1	0.013	*
x_2	1.141×10^{-3}	1	1.141×10^{-3}	7.57	0.0156	*
x_3	3.816×10^{-3}	1	3.816×10^{-3}	25.34	0.0002	***
x_4	2.760×10^{-3}	1	2.760×10^{-3}	18.32	0.0008	***
x_1x_2	9.025×10^{-5}	1	9.025×10^{-5}	0.6	0.4518	
x_1x_3	9.610×10^{-4}	1	9.610×10^{-4}	6.38	0.0242	*
x_1x_4	4.000×10^{-6}	1	4.000×10^{-6}	0.027	0.8729	
x_2x_3	3.610×10^{-4}	1	3.610×10^{-4}	2.4	0.1439	
x_2x_4	1.210×10^{-4}	1	1.210×10^{-4}	0.8	0.3853	
x_3x_4	9.000×10^{-6}	1	9.000×10^{-6}	0.06	0.8104	
x_1^2	0.010	1	0.010	67.41	< 0.0001	***
x_2^2	0.014	1	0.014	95.39	< 0.0001	***
x_3^2	0.021	1	0.021	142.08	< 0.0001	***
x_4^2	7.694×10^{-3}	1	7.694×10^{-3}	51.08	< 0.0001	***
Residual	2.109×10^{-3}	14	1.506×10^{-4}			
Lack of Fit	1.912×10^{-3}	10	1.912×10^{-4}	3.89	0.1014	
Pure Error	1.968×10^{-4}	4	4.920×10^{-5}			
Cor Total	0.048	28				
	$R^2 = 0.9560$	Adeq.Precision = 13.978				

Sig. significant level, * Significant at 0.05 level, ** Significant at 0.01 level, *** Significant at 0.001 level.
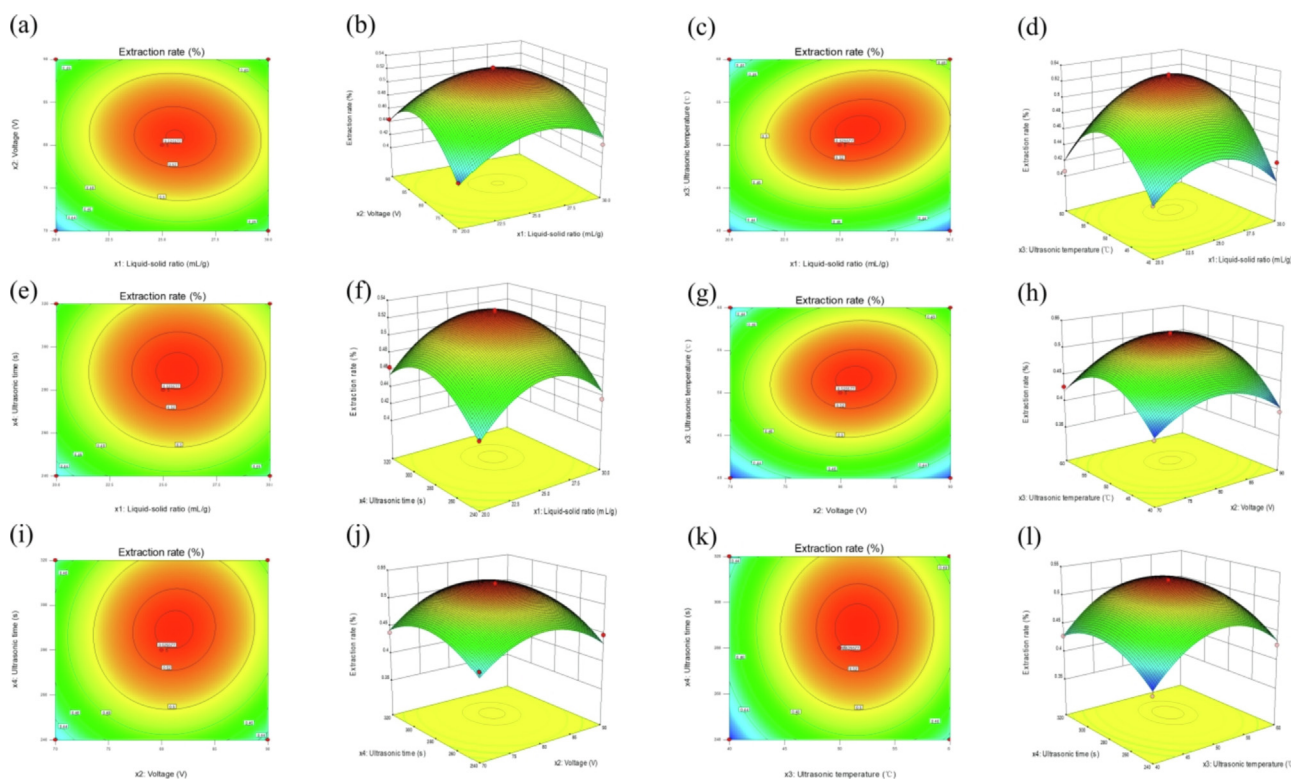
Fig. 1 Two-dimensional contour plots (a, c, e, g, i, k) and response surface plots (b, d, f, h, j, l) showing the effect of liquid–solid ratio, voltage, ultrasonic temperature and ultrasonic time on the extraction rates of PCMR.

as shown in Fig. 1(c). In contrast, the interaction of the other two factors was insignificant.

3.1.3. Verification experiments

The ideal extraction conditions to obtain the maximum extraction rate of PCMR from regression Eq. (8) were: liquid–solid ratio 25.8:1 (mL/g), voltage 81.0 V, ultrasonic temperature 51.8 °C, and ultrasonic time 289 s. The expected extraction rate was 0.529%. Under these extraction process conditions, the PCMR extraction rate was $0.531 \pm 0.004\%$, which was consistent with the predicted values, suggesting that the model was appropriate for the extraction process described above.

3.2. Purification of PCMR

The AB-8 macroporous resin has been reported in many previous studies to have physicochemical stability, adsorption/desorption selectivity and recoverability and is now widely used for the purification of plant phenols (Cui et al., 2018; Hamed et al., 2019). The purification of phenolics from sweet potato leaves with AB-8 macroporous resin has been reported to be efficient, economical and environmentally friendly, with great potential for industrial production (Xi et al., 2015). In this study, the contents of total phenols, flavonoids, flavonols, flavanols and phenolic acids were analysed by UV–Vis spectrophotometry before and after purification, as shown in Table 3, where AB-8 macroporous resin performs well in PCMR purification. The purities of total phenolics, flavonoids, flavonols, flavanols and phenolic acids were significantly improved, which indicated that AB-8 macroporous resin was an ideal purification medium with high separation efficiency.

3.3. Antioxidant activities

Common methods used to evaluate antioxidant capacity are DPPH, ABTS$^+$ and superoxide anion radical scavenging assays. The DPPH radical scavenging capacity assay is widely used to test the antioxidant capacity of various antioxidant samples because of its simplicity, rapidity and sensitivity. The ABTS$^+$ radical scavenging capacity assay is commonly

Table 3 The contents of total phenolics, flavonoids, flavonols, flavanols and phenolic acids in PPCMR before and after AB-8 resin purification.

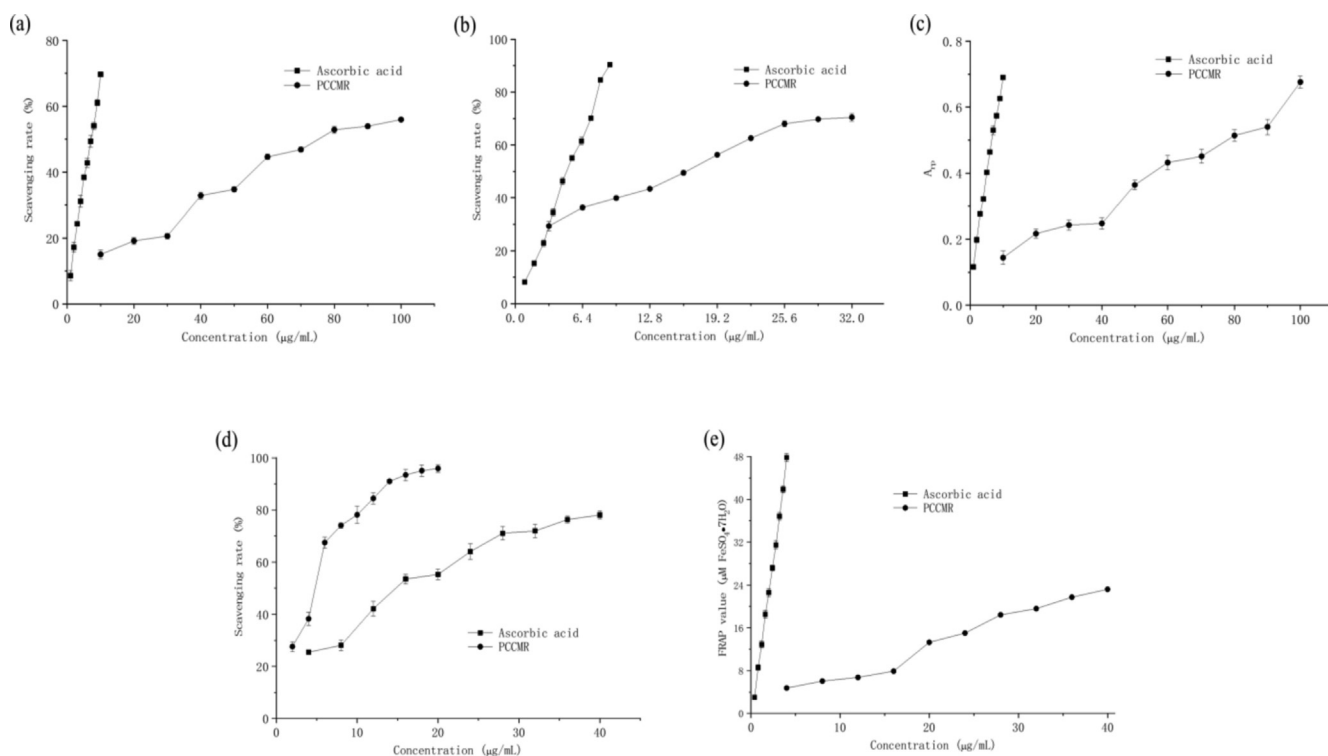| Measurement	Before purification	After purification	Multiplication of content after purification
Total phenolics (mg GAE/g)	79.90 ± 0.98	263.6 ± 0.70	2.30
Total flavonoids(mg RE/g)	74. 20 ± 1.46	272.0 ± 1.68	2.67
Total flavonols (mg RE/g)	29.20 ± 0.88	104.7 ± 0.89	2.59
Total flavanols (mg CE/g)	4.790 ± 0.10	22.21 ± 0.34	3.63
Total phenolic acids(mg CAE/g)	47.75 ± 1.45	184.4 ± 2.03	2.86

Fig. 2 Antioxidant activities of PPCMR. (a) DPPH radical scavenging activities; (b) ABTS$^+$ radical scavenging activities; (c) Superoxide anion radical scavenging activities; (d) RP activities and (e) FRAP activities. Ascorbic acid was used as a positive control. Each value is presented as mean $\pm$ SD (n = 3).
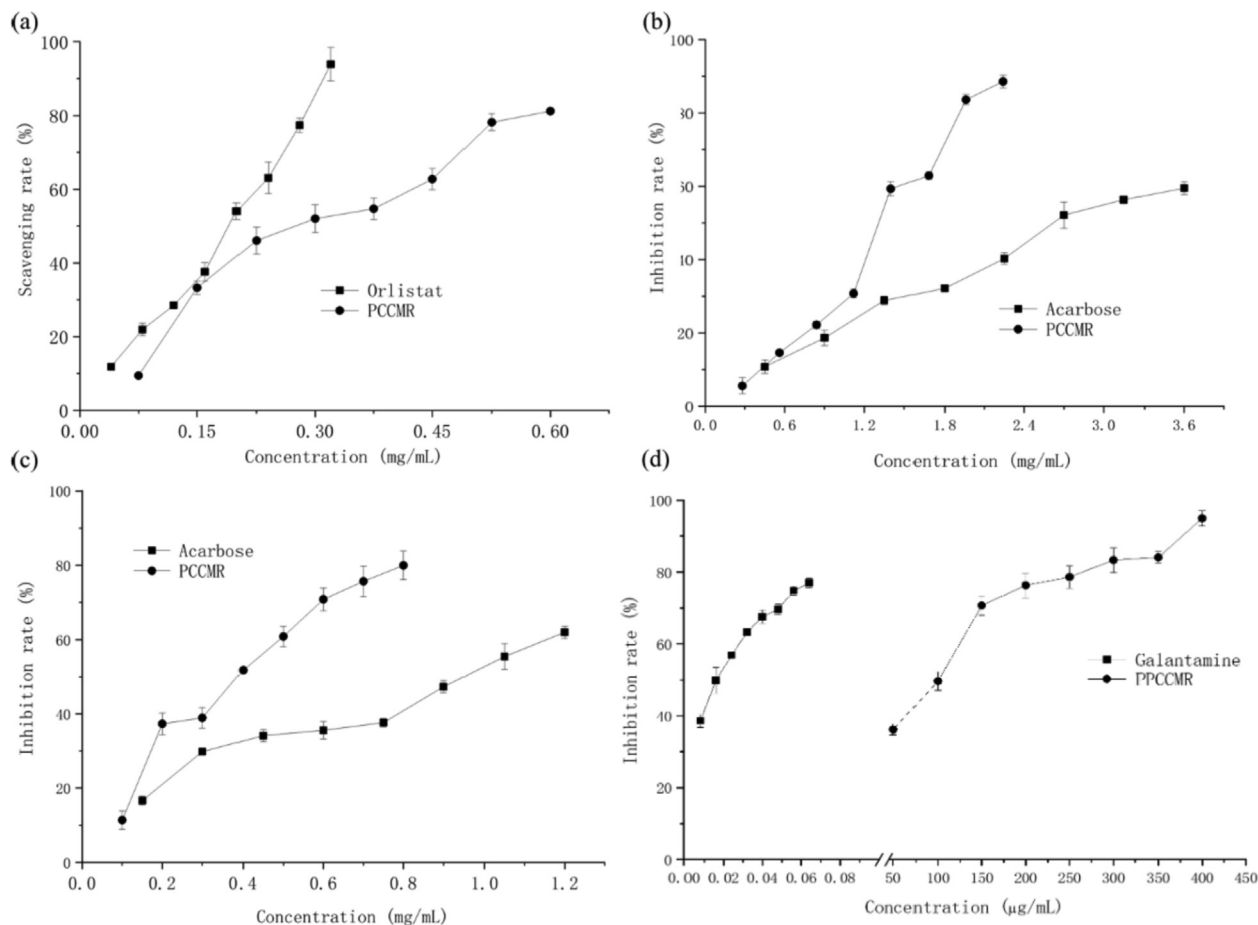

Fig. 3 Enzyme inhibitory activities of PPCMR. (a) Lipase inhibitory activities; (b) α-amylase inhibitory activities; (c) α-glucosidase inhibitor activities; (d) Acetylcholinesterase inhibitory activities. Each value is presented as mean $\pm$ SD (n = 3).

used to assess the total antioxidant capacity of different active substances. The superoxide anion assay uses NADH-PMS-NBT as a superoxide anion (O_2^-) generating system to detect the reducing capacity of reducing substances in the system. All of these reflect the ability of the sample to provide hydrogen atoms and block free radical chain reactions (Mohamed et al., 2019; Pérez-Jiménez et al., 2007). It could be seen from Fig. 2(a-c) that with the increase of the concentrations of PPCMR, the scavenging rates of DPPH, $ABTS^+$ and superoxide anion radicals gradually increased, and there was a certain dose–response relationship between them. The SC_{50} values of PPCMR for DPPH, $ABTS^+$ and superoxide anion radical scavenging activities were 80.32, 12.89 and 14.27 µg/mL, respectively and the SC_{50} values of ascorbic acid were 6.74, 4.48 and 4.24 µg/mL, respectively. This indicated that DPPH, $ABTS^+$ and superoxide anion radicals scavenging activities of PPCMR were weaker than those of ascorbic acid, but this does not affect them as effective free radical scavengers. In previous studies, the researchers got the similar results. They concluded that the derivatives from *Morus alba* root bark showed good antioxidant activity in DPPH and $ONOO^-$ scavenging assays (Muanda et al., 2010; Paudel et al., 2020). The RP and FRAP analysis reflected the capacity of the sample to decrease potas-

sium (Fe^{3+}) to potassium ferrocyanide (Fe^{2+}) and TPTZ-Fe (III) to TPTZ-Fe(II) (Sokamte et al., 2019; Yang et al., 2011). Both assays could be used as indicators to assess potential antioxidant properties. As illustrated in Fig. 2(d-e), with the increase of the concentrations of PPCMR, the A_{rp} and A_{frap} values of PPCMR gradually increased, and there was a certain dose–response relationship between them. However, the RP and FRAP activities of PPCMR were lower than those of ascorbic acid, which implied that ascorbic acid possessed a stronger effect. But this couldn't prevent PPCMR from becoming a good natural antioxidant. Furthermore, our findings were corresponding to the previous reports (Abdel-Haleem et al., 2017; Murugan and Parimelazhagan, 2014).

3.4. Enzyme inhibitory activities

Lipase is involved in the metabolism of triglycerides, and is the basic enzyme for lipid hydrolysis (Spínola et al., 2020). Hyperlipidemia arises from excessive lipase activity, producing too much monoglycerides and fatty acids. Lipase inhibitors promote the elimination of lipids from the body by reducing the amount of lipid hydrolysates, which leads to weight loss. α-
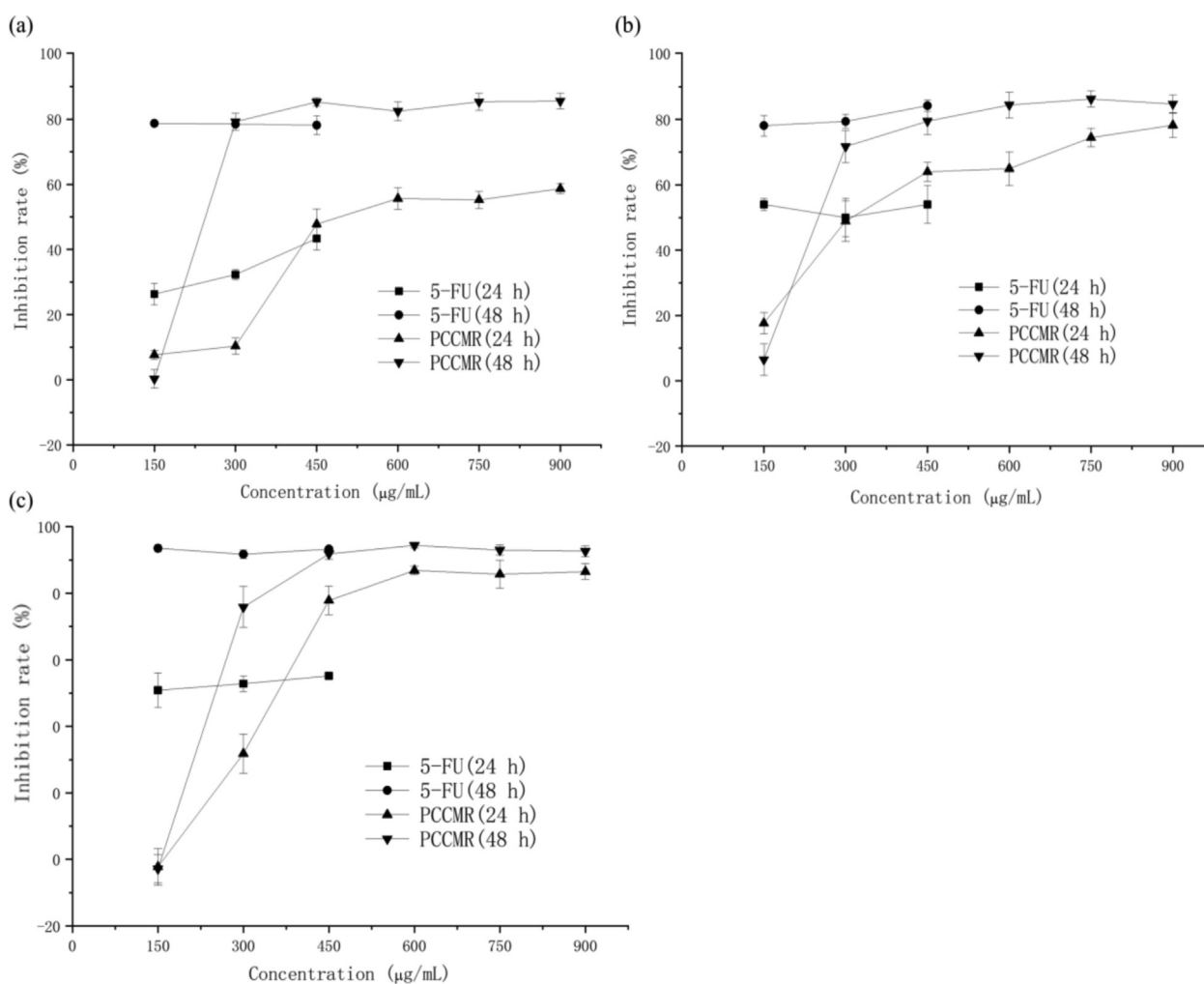

Fig. 4 Antiproliferative activities of PPCMR. (a) Human cervical cancer Hela cell inhibiting activities; (b) Human hepatoma HepG2 cell inhibiting activities; (c) Human lung cancer NCI-H460 cell inhibiting activities. Each value is presented as mean ± SD (n = 3).

amylase and α-glucosidase are considered therapeutic targets for the regulation of postprandial hyperglycemia (Jonathan et al., 2018; Young et al., 2010). Acetylcholinesterase is a neurotransmitter hydrolase that rapidly hydrolyzes acetylcholine at choline synapses, preventing acetylcholine accumulation and maintaining normal physiological function of the nervous system (Oliveira et al., 2011; Masuoka et al., 2019). Future treatment of Alzheimer's disease by inhibition of acetylcholinesterase is expected and may be used to treat Parkinson's disease, aging, and myasthenia gravis (Bianco et al., 2015; Masondo et al., 2018). The inhibitory activities of PPCMR against lipase, α-amylase, α-glucosidase and acetylcholinesterase were presented in Fig. 3(a-d). The PPCMR within the selected concentration range could inhibit the enzyme activities dose-dependently. The IC_{50} values of PPCMR against lipase, α-amylase, α-glucosidase and acetylcholinesterase were 0.27 mg/mL, 1.25 mg/mL, 0.35 mg/mL and 85.18 μg/mL, respectively. However, the IC_{50} values of the positive controls (orlistat, acarbose, acarbose and galantamine) were 0.16 mg/mL, 2.76 mg/mL, 0.94 mg/mL, 0.016 μg/mL, respectively. The results showed that there were only a few differences of inhibition effect between the PPCMR and the positive controls on lipase, α-amylase, α-glucosidase. However, the inhibition effect of PPCMR on acetylcholinesterase was more than five thousand times lower than that of galantamine. Thus, the experimental results indicated that PPCMR had remarkable inhibition effects on lipase, α-amylase and α-glucosidase activities, but their inhibition effect on acetyl-cholinesterase activity was comparatively ineffective. According to the literatures, the results were similar to earlier studies. Cortex Mori's prenylated flavonoids, flavonols and alkaloids are small molecule α-glucosidase inhibitory components, and its flavonoid derivatives could significantly inhibit on pancreatic lipase activities (Akhter et al., 2013; Ha et al., 2018; Liu et al., 2013; Hou et al., 2018; Chen et al., 2018; Sadeer et al., 2019).

3.5. Antiproliferative activities

It is one of the important methods to find high specific anticancer drugs to evaluate the anticancer performance using cancer cell lines in *vitro* (Irshad et al., 2014). MTT assay and other detection methods based on tetrazolium haline are the most popular techniques for quantitative assessment of cell proliferation, viability and cytotoxicity (Tim, 1983). Its mechanism is to reduce exogenous MTT to water-insoluble blue purple formazine crystals through succinate dehydrogenase in mitochondria of living cells, nevertheless dead cells have no such function (Zhu et al., 2013). The antiproliferative activities of PPCMR against HeLa, HepG2 and NCI-H460 were presented in Fig. 4(a-c). The antiproliferative activities of PPCMR increased with the increase of the concentrations in both 24 and 48 h of incubation time When the concentrations increased from 150 to 900 μg/mL, the inhibition rates of 24 h of PPCMR treatment ranged from 7.670 ± 1.33% to 58.67 ± 1.53%, 17.66 ± 3.29% to 78.25 ± 3.80%, −2.21 ± 5.53% to 86.49 ± 2.38%, and of 48 h of PPCMR treatment ranged from 0.28 ± 2.78% to 85.57 ± 2.42%, 6.50 ± 4.87% to 84.73 ± 2.81%, −2.79 ± 4.17% to 92.65 ± 1.60%, for the HeLa, HepG2 and NCI-H460 cells, respectively. In general, the result of 48 h treatment was better than that of the 24 h treatment. Similar outcomes were also reported previously (Lu et al., 2018).

3.6. Cellular morphology

Cell morphology is a common indicator of the physiological and growth status of cells. The physiological and growth status
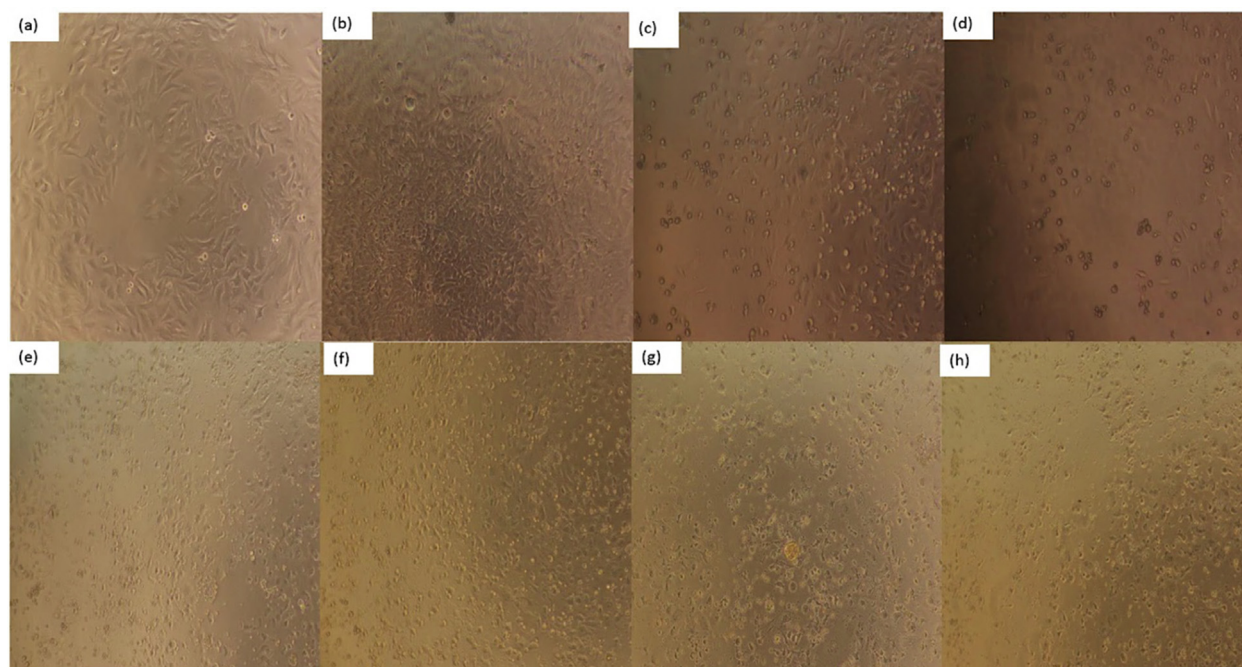

Fig. 5 Effect of PPCMR on morphology of HeLa cells. (a) Negative control group (24 h); (b) Negative control group (48 h); (c) 150 μg/mL 5-FU treatment group (24 h); (d) 150 μg/mL 5-FU treatment group (48 h); (e) 750 μg/mL PPCMR treatment group (24 h); (f) 750 μg/mL PPCMR treatment group (48 h); (g) 900 μg/mL PPCMR treatment group (24 h); (h) 900 μg/mL PPCMR treatment group (48 h).
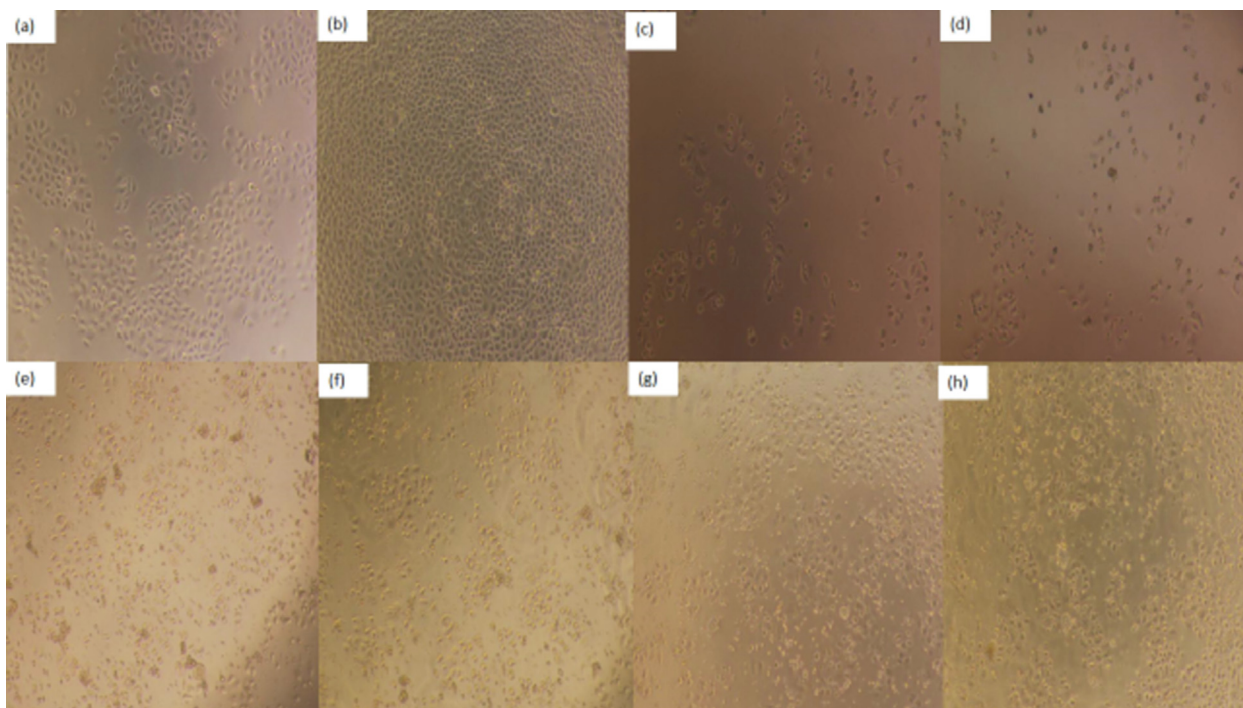
Fig. 6 Effect of PPCMR on morphology of HepG2 cells. (a) Negative control group (24 h); (b) Negative control group (48 h); (c) 150 μg/mL 5-FU treatment group (24 h); (d) 150 μg/mL 5-FU treatment group (48 h). (e) 750 μg/mL PPCMR treatment group (24 h); (f) 750 μg/mL PPCMR treatment group (48 h); (g) 900 μg/mL PPCMR treatment group (24 h); (h) 900 μg/mL PPCMR treatment group (48 h).
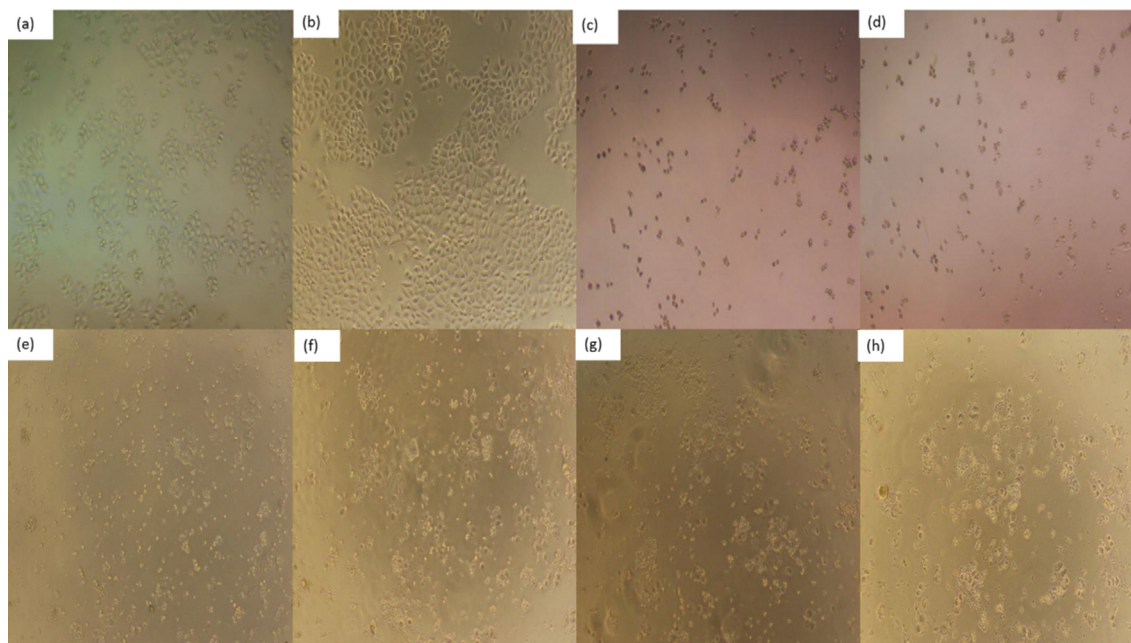

Fig. 7 Effect of PPCMR on morphology of NCIH460 cells. (a) Negative control group (24 h); (b) Negative control group (48 h); (c) 150 μg/mL 5-FU treatment group (24 h); (d) 150 μg/mL 5-FU treatment group (48 h); (e) 750 μg/mL PPCMR treatment group (24 h); (f) 750 μg/mL PPCMR treatment group (48 h); (g) 900 μg/mL PPCMR treatment group (24 h); (h) 900 μg/mL PPCMR treatment group (48 h).

of the cells can be assessed by observation at the morphology of the cells, so as to further reflect the effect of drugs on cell growth (Xiaoqiang et al., 2019). Morphological changes of HeLa, HepG2 and NCI-H460 cells treated or untreated with different concentrations of PPCMR were observed after 24 and 48 h. As shown in Figs. 5–7, PPCMR exhibited antiproliferative on HeLa, HepG2 and NCI-H460 cells in a time and dosage-related manner. According to the model control group, it could be seen that the cells of HeLa, HepG2 and NCIH460 all presented irregular shapes and grew adherent to the inner wall of the culture plate. Especially after the 48 h of culture, the cells were tightly connected, and the cell number increased significantly. However, compared with the model control group, after PPCMR (750 and 900 μg/mL) or 5-FU treatment for 24 and 48 h, the number of adherent cells decreased significantly, the cell morphology changed from an irregular shape to a round shape. At the same time, it could also be seen that 900 μg/mL PPCMR treatment was more effective than that of 750 μg/mL. Collectively, these results suggested that PPCMR effectively inhibits the proliferation of HeLa, HepG2 and NCI-H460 cells in *vitro*. The outcome of the assay was similar to that of the literature, they found that treatment in a dose-dependent manner of Mori Cortex Radicis extracts had the better anti-proliferative activity on Raw 264.7 cells, also speculated that the anti-inflammatory activity may be related to p38-Mitogen-activated protein kinase (MAPK), and Nuclear factor Kappa B (NF-κB) (Seo et al., 2013; Bayazid et al., 2019).

4. Conclusions

In this study, an efficient UTPHSE technique and Box-Behnken design were used to optimize the extraction process of PMCR. The ideal constraints were: liquid–solid ratio 25.8:1 (mL/g), voltage 81.0 V, ultrasonic temperature 51.8 ℃ and ultrasonic time 289 s. Under these conditions of the extraction process, the experimental extraction rate was 0.531 ± 0.004%, which was in good agreement with the predicted value (0.529%), suggesting that the model is suitable for the above extraction process. In this study, we carried out, for the first time, an in-depth assessment of the antioxidant, enzyme (lipase, α-amylase, α-glucosidase and acetyl-cholinesterase) inhibitory and antiproliferative properties of PPCMR. It could be concluded from this research that PPCMR have the potential to be employed as natural antioxidants, or antilipidemic, hypoglycemic or antineoplastic agents in the nutraceutical and pharmaceutical industries, however not suitable to be used as an acetyl-cholinesterase inhibitor. Further studies are needed to elucidate the mechanisms of anti-lipid, hypoglycemic or anti-tumor activity of PPCMR in *vivo*.

Author contributions

Experimental design, analysis, writing-C.L, Y.P, W.T, T.L, J.C and Y.S; data analysis, interpretation, software-C.L, Y.P, W.W, Y.Y and Y.S; final draft, validation, resources- C.L, Y.P, T.L, J. F, J.H and Y.C; visualization, proof reading, funding acquisition-A.M.A, M.K.G, R.A.R. All authors have read the published version of the manuscript and agrees with its contents.

Declaration of Competing Interest

The authors declare that they have no known competing financial interests or personal relationships that could have appeared to influence the work reported in this paper.

Institutional review board statement

Not applicable.

Data availability statement

In the article and manuscript the information referred to in the data used to support the results of this study.

References

Abdel-Haleem, S.A., Ibrahim, A.Y., Ismail, R.F., Shaffie, N.M., Hendawy, S.F., Omer, E.A., 2017. In-vivo hypoglycemic and hypolipidemic properties of Tagetes lucida alcoholic extract in streptozotocin-induced hyperglycemic Wistar albino rats. Ann. Agric. Sci. 62, 169–181. https://doi.org/10.1016/j.aoas.2017.11.005.

Akhter, F., Hashim, A., Khan, M.S., Ahmad, S., Iqbal, D., Srivastava, A.K., Siddiqui, M.H., 2013. Antioxidant, α-amylase inhibitory and oxidative DNA damage protective property of Boerhaavia diffusa (Linn.) root. S. Afr. J. Bot. 88, 265–272. https://doi.org/10.1016/j.sajb.2013.06.024.

Alcântara, M.A., Polari, I.D.L.B., de Albuquerque Meireles, B.R.L., de Lima, A.E.A., da Silva Junior, J.C., de Andrade Vieira, É., Dos Santos, N.A., de Magalhães Cordeiro, A.M.T., 2019. Effect of the solvent composition on the profile of phenolic compounds extracted from chia seeds. Food Chem. 275, 489–496. https://doi.org/10.1016/j.foodchem.2018.09.133.

Asano, N., Yamashita, T., Yasuda, K., Ikeda, K., Kizu, H., Kameda, Y., Ryu, K.S., 2001. Polyhydroxylated Alkaloids Isolated from Mulberry Trees (Morus alba L.) and Silkworms (Bombyx mori L.). J. Agric. Food. Chem. 49 (9), 4208–4213. https://doi.org/10.1021/jf010567e.

Barak, T.H., Celep, E., İnan, Y., Yesilada, E., 2019. Influence of in vitro human digestion on the bioavailability of phenolic content and antioxidant activity of Viburnum opulus L. (European cranberry) fruit extracts. Ind. Crops Prod. 131, 62–69. https://doi.org/10.1016/j.indcrop.2019.01.037.

Bayazid, A., Kim, J.G., Park, S.H., Lim, B.O., 2019. Antioxidant, antiinflammatory and antiproliferative activity of mori cortex radicis extracts. Nat. Prod. Commun. 1 (15), 1–8. https://doi.org/10.1177/1934578X19899765.

Benabderrahim, M.A., Yahia, Y., Bettaieb, I., Elfalleh, W., Nagaz, K., 2019. Antioxidant activity and phenolic profile of a collection of medicinal plants from Tunisian arid and Saharan regions. Ind. Crops Prod. 138. https://doi.org/10.1016/j.indcrop.2019.05.076.

Bianco, É.M., Krug, J.L., Zimath, P.L., Kroger, A., Paganelli, C.J., Boeder, A.M., Rebelo, R.A., 2015. Antimicrobial (including

antimollicutes), antioxidant and anticholinesterase activities of Brazilian and Spanish marine organisms – evaluation of extracts and pure compounds. Revista Brasileira de Farmacognosia 25 (6), 668–676. https://doi.org/10.1016/j.bjp.2015.07.018.

Blaszczak, W., Jez, M., Szwengiel, A., 2020. Polyphenols and inhibitory effects of crude and purified extracts from tomato varieties on the formation of advanced glycation end products and the activity of angiotensin-converting and acetylcholinesterase enzymes. Food Chem. 314. https://doi.org/10.1016/j.foodchem.2020.126181.

Cătunescu, G.M., Rotar, A.M., Pop, C.R., Diaconeasa, Z., Bunghez, F., Socaciu, M.-I., Semeniuc, C.A., 2018. Influence of extraction pre-treatments on some phytochemicals and biological activity of Transylvanian cranberries (Vaccinium vitis-idea L.). LWT 102, 385–392. https://doi.org/10.1016/j.lwt.2018.12.062.

Chen, Z., Du, X., Yang, Y., Cui, X., Zhang, Z., Li, Y., 2018. Comparative study of chemical composition and active components against α-glucosidase of various medicinal parts of morus alba l. Biomed. Chromatogr. 32 (11). https://doi.org/10.1002/bmc.4328.

Cheng, Z., Zhang, Y., Song, H., Zhou, H., Zhong, F., Hu, H., Feng, Y., 2016. Extraction optimization, characterization and antioxidant activity of polysaccharide from Gentiana scabra bge. Int. J. Biol. Macromol. 93, 369–380. https://doi.org/10.1016/j.ijbiomac.2016.08.059.

Cui, Q., Liu, J.-Z., Wang, L.-T., Kang, Y.-F., Meng, Y., Jiao, J., Fu, Y.-J., 2018. Sustainable deep eutectic solvents preparation and their efficiency in extraction and enrichment of main bioactive flavonoids from sea buckthorn leaves. J. Cleaner Prod. 184, 826–835. https://doi.org/10.1016/j.jclepro.2018.02.295.

Čulenová, M., Sychrová, A., Hassan, S.T.S., Berchová-Bímová, K., Svobodová, P., Helclová, A., Šmejkal, K., 2020. Multiple In vitro biological effects of phenolic compounds from Morus alba root bark. J. Ethnopharmacol. 248. https://doi.org/10.1016/j.jep.2019.112296.

Deghima, A., Righi, N., Rosales-Conrado, N., León-González, M.E., Gómez-Mejía, E., Madrid, Y., Bedjou, F., 2020. Bioactive polyphenols from Ranunculus macrophyllus Desf. Roots: Quantification, identification and antioxidant activity. S. Afr. J. Bot. 132, 204–214. https://doi.org/10.1016/j.sajb.2020.03.036.

Ercisli, S., Orhan, E., 2006. Chemical composition of white (Morus alba), red (Morus rubra) and black (Morus nigra) mulberry fruits. Food Chem. 103 (4), 1380–1384. https://doi.org/10.1016/j.foodchem.2006.10.054.

Ferrari, F., Delle Monache, F., Suarez, A.I., Compagnone, R.S., 2000. Multicaulisin, a new Diels-Alder type adduct from Morus multicaulis. Fitoterapia 71 (2), 213–215. https://doi.org/10.1016/S0367-326X(99)00156-2.

Gali, L., Bedjou, F., 2018. Antioxidant and anticholinesterase effects of the ethanol extract, ethanol extract fractions and total alkaloids from the cultivated Ruta chalepensis. S. Afr. J. Bot. 120, 163–169. https://doi.org/10.1016/j.sajb.2018.04.011.

Garcia-Castello, E.M., Rodriguez-Lopez, A.D., Mayor, L., Ballesteros, R., Conidi, C., Cassano, A., 2015. Optimization of conventional and ultrasound assisted extraction of flavonoids from grapefruit (Citrus paradisi L.) solid wastes. LWT - Food Sci. Technol. 64 (2), 1114–1122. https://doi.org/10.1016/j.lwt.2016.12.001.

Guo, X., Zhao, W., Liao, X., Hu, X., Wu, J., Wang, X., 2017. Extraction of pectin from the peels of pomelo by high-speed shearing homogenization and its characteristics. LWT - Food Sci. Technol. 79, 640–646. https://doi.org/10.1016/j.lwt.2016.12.001.

Gutiérrez-Grijalva, E.P., Antunes-Ricardo, M., Acosta-Estrada, B.A., Gutiérrez-Uribe, J.A., Heredia, J.B., 2019. Cellular antioxidant activity and in vitro inhibition of α-glucosidase, α-amylase and pancreatic lipase of oregano polyphenols under simulated gastrointestinal digestion. Food Res. Int. 116, 676–686. https://doi.org/10.1016/j.foodres.2018.08.096.

Ha, M.T., Seong, S.H., Nguyen, T.D., Cho, W.-K., Ah, K.J., Ma, J.Y., Min, B.S., 2018. Chalcone derivatives from the root bark of Morus alba L. act as inhibitors of PTP1B and α -glucosidase. Phytochemistry 155, 114–125. https://doi.org/10.1016/j.phytochem.2018.08.001.

Hamed, Y.S., Abdin, M., Akhtar, H.M.S., Chen, D., Wan, P., Chen, G., Zeng, X., 2019. Extraction, purification by macrospores resin and in vitro antioxidant activity of flavonoids from Moringa oliefera leaves. S. Afr. J. Bot. 124, 270–279. https://doi.org/10.1016/j.sajb.2019.05.006.

Hisato, K., Ryo, T., Yukio, S., 2008. Localization of mucilaginous polysaccharides in mulberry leaves. Protoplasma 233 (1–2), 3627–3634. https://doi.org/10.1002/jssc.200900348.

Hou, X.D., Ge, G.B., Weng, Z.M., Dai, Z.R., Leng, Y.H., Ding, L.L., et al, 2018. Natural constituents from cortex mori radicis as new pancreatic lipase inhibitors. Bioorg. Chem. 80, 577–584. https://doi.org/10.1016/j.bioorg.2018.07.011.

Hu, Y., Xu, J., Chen, Q., Liu, M., Wang, S., Yu, H., Wang, T., 2020. Regulation effects of total flavonoids in Morus alba L. on hepatic cholesterol disorders in orotic acid induced NAFLD rats. BMC Complem. Med. Ther. 20 (1), 257. https://doi.org/10.1186/s12906-020-03052-w.

Huang, G., Zeng, Y., Wei, L., Yao, Y., Dai, J., Liu, G., Gui, Z., 2020. Comparative transcriptome analysis of mulberry reveals anthocyanin biosynthesis mechanisms in black (Morus atropurpurea Roxb.) and white (Morus alba L.) fruit genotypes. BMC Plant Biol. 20 (1). https://doi.org/10.1186/s12870-020-02486-1.

Imran, M., Khan, H., Shah, M., Khan, R., Khan, F., 2010. Chemical composition and antioxidant activity of certain Morus species. J. Zhejiang Univ. Sci. B 11 (12), 973–980. doi: CNKI:SUN:ZDYW.0.2010-12-012.

Irshad, M., Ahmad, I., Mehdi, S.J., Goel, H.C., Rizvi, M.M.A., 2014. Antioxidant Capacity and Phenolic Content of the Aqueous Extract of Commonly Consumed Cucurbits. Int. J. Food Prop. 17 (1), 179–186. https://doi.org/10.1080/10942912.2011.619025.

Jiao, Y., Chen, D., Fan, M., Quek, S.Y., 2018. UPLC-QqQ-MS/MS-based phenolic quantification and antioxidant activity assessment for thinned young kiwifruits. Food Chem. 281, 97–105. https://doi.org/10.1016/j.foodchem.2018.12.062.

Jonathan, B., Scott, D., Gianluca, R., Diane, N., Jose, F., 2018. Treatment with Herbal Mouthwash Mediates Improvement of Symptoms in Xerostomia and Oral Mucositis patients. J. Nutrit. Biol. 4 (2), 202–206. https://doi.org/10.18314/jnb.v4i2.1060.

Kim, H.-J., Lee, H.J., Jeong, S.-J., Lee, H.-J., Kim, S.-H., Park, E.-J., 2011. Cortex Mori Radicis extract exerts antiasthmatic effects via enhancement of CD4 + CD25 + Foxp3 + regulatory T cells and inhibition of Th2 cytokines in a mouse asthma model. J. Ethnopharmacol. 138 (1), 40–46. https://doi.org/10.1016/j.jep.2011.08.021.

Lei, X., Hu, W.-B., Yang, Z.-W., Hui-Chen, Wang-Ning, Liu-Xin, , Wang, W.-J., 2019. Enzymolysis-ultrasonic assisted extraction of flavanoid from Cyclocarya paliurus (Batal) Iljinskaja: HPLC profile, antimicrobial and antioxidant activity. Ind. Crops Prod. 130, 615–626. https://doi.org/10.1016/j.indcrop.2019.01.027.

Lin, T., Liu, Y., Lai, C., Yang, T., Xie, J., Zhang, Y., 2018. The effect of ultrasound assisted extraction on structural composition, antioxidant activity and immunoregulation of polysaccharides from Ziziphus jujuba Mill var. spinosa seeds. Ind. Crops Prod. 125, 150–159. https://doi.org/10.1016/j.indcrop.2018.08.078.

Liu, S., Li, D., Huang, B., Chen, Y., Lu, X., Wang, Y., 2013. Inhibition of pancreatic lipase, alpha-glucosidase, alpha-amylase, and hypolipidemic effects of the total flavonoids from Nelumbo nucifera leaves. J. Ethnopharmacol. 149 (1), 263–269. https://doi.org/10.1016/j.jep.2013.06.034.

Liu, Z., Yang, L., 2018. Antisolvent precipitation for the preparation of high polymeric procyanidin nanoparticles under ultrasonication and evaluation of their antioxidant activity in vitro. Ultrason.

Sonochem. 43, 208–218. https://doi.org/10.1016/j.ultsonch.2018.01.019.

Lu, C., Li, C., Chen, B., Shen, Y., 2018. Composition and antioxidant, antibacterial, and anti-HepG2 cell activities of polyphenols from seed coat of Amygdalus pedunculata Pall. Food Chem. 265, 111–119. https://doi.org/10.1016/j.foodchem.2018.05.091.

Masondo, N.A., Stafford, G.I., Aremu, A.O., Makunga, N.P., 2018. Acetylcholinesterase inhibitors from southern African plants: An overview of ethnobotanical, pharmacological potential and phytochemical research including and beyond Alzheimer's disease treatment. S. Afr. J. Bot. 120, 39–64. https://doi.org/10.1016/j.sajb.2018.09.011.

Masuoka, T., Uwada, J., Kudo, M., Yoshiki, H., Yamashita, Y., Taniguchi, T., Muramatsu, I., 2019. Augmentation of Endogenous Acetylcholine Uptake and Cholinergic Facilitation of Hippocampal Long-Term Potentiation by Acetylcholinesterase Inhibition. Neuroscience 404, 39–64. https://doi.org/10.1016/j.neuroscience.2019.01.042.

Mohamed, H., Marwa, H., Sabrine, S., Ghada, K., Hocine, L., Suming, L., Moncef, N., 2019. Structural characterization, antioxidant and antibacterial activities of a novel polysaccharide from Periploca laevigata root barks. Carbohydr. Polym. 206, 380–388. https://doi.org/10.1016/j.carbpol.2018.11.020.

Muanda, F.N., Dicko, A., Soulimani, R., 2010. Assessment of polyphenolic compounds, in vitro antioxidant and anti-inflammation properties of Securidaca longepedunculata root barks. Comptes rendus - Biologies 333 (9), 663–669. https://doi.org/10.1016/j.crvi.2010-07.002.

Murugan, R., Parimelazhagan, T., 2014. Comparative evaluation of different extraction methods for antioxidant and anti-inflammatory properties from Osbeckia parvifolia Arn. – An in vitro approach. J. King Saud Univ. – Sci. 26 (4), 267–275. https://doi.org/10.1016/j.jksus.2013.09.006.

Oliveira, R.D.L., Seibt, K.J., Rico, E.P., Bogo, M.R., Bonan, C.D., 2011. Inhibitory effect of lithium on nucleotide hydrolysis and acetylcholinesterase activity in zebrafish (Danio rerio) brain. Neurotoxicol. Teratol. 33 (6).

Oyedeji-Amusa, M.O., Ashafa, A.O.T., 2019. Medicinal properties of whole fruit extracts of Nauclea latifolia Smith. Antimicrobial, antioxidant and hypoglycemic assessments. S. Afr. J. Bot. 121, 651–657. https://doi.org/10.1016/j.ntt.2011.05.005.

Paola, D., Paola, D., Francesco, C., Paola, G.M., Antonio, R., Luigi, M., 2009. Characterization of the polyphenolic fraction of Morus alba leaves extracts by HPLC coupled to a hybrid IT-TOF MS system. J. Sep. Sci. 32 (21), 3627–3634. https://doi.org/10.1002/jssc.200900348.

Paudel, P., Seong, S.H., Wagle, A., Min, B.S., Jung, H.A., Choi, J.S., 2020. Antioxidant and anti-browning property of 2-arylbenzofuran derivatives from Morus alba Linn root bark. Food Chem. 309. https://doi.org/10.1016/j.foodchem.2019.125739.

Pérez-Jiménez, J., Arranz, S., Tabernero, M., Rubio, M.E.D., Serrano, J., Goñi, I., Saura-Calixto, F., 2007. Updated methodology to determine antioxidant capacity in plant foods, oils and beverages: Extraction, measurement and expression of results. Food Res. Int. 41 (3), 274–285. https://doi.org/10.1016/j.foodres.2007.12.004.

Rao, P.R., Rathod, V.K., 2015. Mapping study of an ultrasonic bath for the extraction of andrographolide from Andrographis paniculata using ultrasound. Ind. Crops Prod. 66, 312–318. https://doi.org/10.1016/j.indcrop.2014.11.046.

Sadeer, N.B., Llorent-Martínez, E.J., Bene, K., Mahomoodally, M.F., Mollica, A., Sinan, K.I., Zengin, G., 2019. Chemical profiling, antioxidant, enzyme inhibitory and molecular modelling studies on the leaves and stem bark extracts of three African medicinal plants. J. Pharm. Biomed. Anal. 174, 19–33. https://doi.org/10.1016/j.jpba.2019.05.041.

Seo, C.S., Lim, H.S., Jeong, S.J., Ha, H., Shin, H.K., 2013. Hplc-pda analysis and anti-inflammatory effects of mori cortex radicis. Nat.

Prod. Commun. 8 (10), 1443–1446. https://doi.org/10.1177/1934578X1300801027.

Shibata, Y., Kume, N., Arai, H., Hayashida, K., Inui-Hayashida, A., Minami, M., Yokode, M., 2007. Mulberry leaf aqueous fractions inhibit TNF-alpha-induced nuclear factor kappaB (NF-kappaB) activation and lectin-like oxidized LDL receptor-1 (LOX-1) expression in vascular endothelial cells. Atherosclerosis 193 (1), 20–27. https://doi.org/10.1016/j.atherosclerosis.2006.08.011.

Sokamte, T.A., Mbougueng, P.D., Tatsadjieu, N.L., Sachindra, N.M., 2019. Phenolic compounds characterization and antioxidant activities of selected spices from Cameroon. S. Afr. J. Bot. 121, 7–15. https://doi.org/10.1016/j.sajb.2018.10.016.

Song, Q., Xia, X., Ji, C., Chen, D., Lu, Y., 2019. Optimized flash extraction and UPLC-MS analysis on antioxidant compositions of Nitraria sibirica fruit. J. Pharm. Biomed. Anal. 172, 379–387. https://doi.org/10.1016/j.jpba.2019.05.014.

Spínola, V., Llorent-Martínez, E.J., Castilho, P.C., 2020. Inhibition of α-amylase, α-glucosidase and pancreatic lipase by phenolic compounds of Rumex maderensis (Madeira sorrel). Influence of simulated gastrointestinal digestion on hyperglycaemia-related damage linked with aldose reductase activity and protein glycation. LWT 118 (C), 108727. https://doi.org/10.1016/j.lwt.2019.108727.

Syah, Y., Achmad, S., Ghisalberti, E., Hakim, E., Makmur, L., Soekamto, N., 2004. A stilbene dimer, andalasin B, from the root trunk of Morus macroura. J. Chem. Res. 339–340. https://doi.org/10.3184/0308234041639692.

Teh, S.-S., Birch, E.J., 2014. Effect of ultrasonic treatment on the polyphenol content and antioxidant capacity of extract from defatted hemp, flax and canola seed cakes. Ultrason. Sonochem. 21 (1), 346–353. https://doi.org/10.1016/j.ultsonch.2013.08.002.

Tian, G., Xi, Y., Fangting, B., Dan, L., Ting, Z., Jiangtao, Z., Yurong, G., 2020. Young apple polyphenols as natural α-glucosidase inhibitors: In vitro and in silico studies. Bioorg. Chem. 96. https://doi.org/10.1016/j.bioorg.2020.103625.

Tim, M., 1983. Rapid colorimetric assay for cellular growth and survival: Application to proliferation and cytotoxicity assays. J. Immunol. Methods 65 (1–2), 55–63. https://doi.org/10.1016/0022-1759(83)90303-4.

Wu, Y.X., Kim, Y.J., Kwon, T.H., Tan, C.P., Son, K.H., Kim, T., 2020. Anti-inflammatory effects of mulberry (Morus alba L.) root bark and its active compounds. Nat. Prod. Res. 34 (12), 1786–1790. https://doi.org/10.1080/14786419.2018.1527832.

Xi, L., Mu, T., Sun, H., 2015. Preparative purification of polyphenols from sweet potato (Ipomoea batatas L.) leaves by AB-8 macroporous resins. Food Chem. 172, 166–174. https://doi.org/10.1016/j.foodchem.2014.09.039.

Xiang, Q., Liu, X., Liu, S., Ma, Y., Xu, C., Bai, Y., 2019. Effect of plasma-activated water on microbial quality and physicochemical characteristics of mung bean sprouts. Innovat. Food Sci. Emerg. Technol. 52, 243–249. https://doi.org/10.1016/j.ifset.2018.11.012.

Xiaoqiang, C., Jianchun, X., Wei, H., Shengrong, S., Zhengqi, W., Long, W., Qian, L., 2019. Comparative analysis of physicochemical characteristics of green tea polysaccharide conjugates and its decolored fraction and their effect on HepG2 cell proliferation. Ind. Crops Prod. 131, 243–249. https://doi.org/10.1016/j.indcrop.2019.01.061.

Yan, Z., Luo, X., Cong, J., Zhang, H., Ma, H., Duan, Y., 2019. Subcritical water extraction, identification and antiproliferation ability on HepG2 of polyphenols from lotus seed epicarp. Ind. Crops Prod. 129, 472–479. https://doi.org/10.1016/j.indcrop.2018.12.031.

Yang, Y., Liu, D., Wu, J., Chen, Y., Wang, S., 2011. In vitro antioxidant activities of sulfated polysaccharide fractions extracted from Corallina officinalis. Int. J. Biol. Macromol. 49 (5), 1031–1037. https://doi.org/10.1016/j.ijbiomac.2011.08.026.

Yang, J., Qiu, J., Hu, Y., Zhang, Y., Chen, L., Long, Q., Hao, X., 2019. A natural small molecule induces megakaryocytic differentiation and suppresses leukemogenesis through activation of PKCdelta/ERK1/2

signaling pathway in erythroleukemia cells. Biomed. Pharmacother. 118. https://doi.org/10.1016/j.biopha.2019.109265.

Yang, X., Yang, L., Zheng, H., 2010. Hypolipidemic and antioxidant effects of mulberry (Morus alba L.) fruit in hyperlipidaemia rats. Food Chem. Toxicol. 48 (8), 2374–2379. https://doi.org/10.1016/j.fct.2010.05.074.

Young, K.K., Han, N.T., Hideyuki, K., Moo, K.S., 2010. Alpha-glucosidase inhibitory activity of bromophenol purified from the red alga Polyopes lancifolia. J. Food Sci. 75 (5).

Yuan, Y., Zhang, J., Fan, J., Clark, J., Shen, P., Li, Y., Zhang, C., 2018. Microwave assisted extraction of phenolic compounds from four economic brown macroalgae species and evaluation of their antioxidant activities and inhibitory effects on α-amylase, α-glucosidase, pancreatic lipase and tyrosinase. Food Res. Int. 113, 288–297. https://doi.org/10.1016/j.foodres.2018.07.021.

Zdunić, G., Aradski, A.A., Gođevac, D., Živković, J., Laušević, S.D., Milošević, D.K., Šavikin, K., 2020. In vitro hypoglycemic, antioxidant and anti-neuro degenerative activity of chokeberry (Aronia melanocarpa) leaves. Ind. Crops Prod. 148. https://doi.org/10.1016/j.indcrop.2020.112328.

Zhang, L., Xu, Q., Li, L., Lin, L., Yu, J., Zhu, J., Zang, H., 2020. Antioxidant and enzyme-inhibitory activity of extracts from Erigeron annuus flower. Ind. Crops Prod. 148. https://doi.org/10.1016/j.indcrop.2020.112283.

Zheng, Z.-P., Cheng, K.-W., Zhu, Q., Wang, X.-C., Lin, Z.-X., Wang, M., 2010. Tyrosinase Inhibitory Constituents from the Roots of Morus nigra: A Structure−Activity Relationship Study. J. Agric. Food. Chem. 58 (9), 5368–5373. https://doi.org/10.1021/jf1003607.

Zhong, M., Huang, S., Wang, H., Huang, Y., Xu, J., Zhang, L., 2019. Optimization of ultrasonic-assisted extraction of pigment from Dioscorea cirrhosa by response surface methodology and evaluation of its stability. RSC Adv. 9 (3), 1576–1585. https://doi.org/10.1039/c8ra07455k.

Zhu, M.-L., Liang, X.-L., Zhao, L.-J., Liao, Z.-G., Zhao, G.-W., Cao, Y.-C., Luo, Y., 2013. Elucidation of the transport mechanism of baicalin and the influence of a Radix Angelicae Dahuricae extract on the absorption of baicalin in a Caco-2 cell monolayer model. J. Ethnopharmacol. 150 (2), 553–1539. https://doi.org/10.1016/j.jep.2013.09.011.

Zou, D., Jin, Y., Li, J., Cao, Y., Li, X., 2017. Emulsification solvent extraction of phosphoric acid by tri-n-butyl phosphate using a high-speed shearing machine. Sep. Purif. Technol. 172, 242–250. https://doi.org/10.1016/j.seppur.2016.08.014.